Analysis and Implementation of an Adaptive Algorithm for the Rejection of Multiple Sinusoidal Disturbances*

Xiuyan Guo† and Marc Bodson‡

January 27, 2008

Abstract

A discrete-time adaptive algorithm is proposed to reject periodic disturbances in the case where the frequencies are unknown and a reference sensor is not available. The stability of the algorithm is analyzed using averaging theory, and the design of the parameters is based on the linearized averaged system. While the algorithm is first designed for rejecting periodic disturbances with one sinusoidal component, it is also extended to deal with cases where the disturbance has multiple sinusoidal components. A frequency separation method is proposed to prevent the frequency estimates from converging to the same value. The effectiveness of the adaptive scheme is validated in simulations and in experiments on an active noise control testbed.

Index Terms—active noise control, adaptive control, averaging analysis, magnitude phase-locked loop, periodic disturbance rejection.

1 Introduction

Many engineering systems are subjected to periodic disturbances that adversely affect the performance and operation of the systems. For example, in a computer disk drive system, the positioning

*This material is based upon work supported by the National Science Foundation under Grant No. ECS0115070.

†X. Guo is with QSecure, 333 Distel Cir, Los Altos, CA, 94022, USA(email: xguo@qsecure.com)

‡M. Bodson is with the Department of Electrical and Computer Engineering, University of Utah, 50 S Central Campus Dr Rm 3280, Salt Lake City, UT 84112, USA (email: bodson@ece.utah.edu).

of the read/write head is performed by a servo system. A repeatable runout error is caused by the eccentricity of the track and must be compensated for [22] [25]. In *active noise control* (ANC), the main objective is to eliminate or significantly reduce noise generated by a so-called "primary" source. The primary source is often a rotating machine producing a periodic noise. Reduction of the noise level is performed by a "secondary" source (usually loudspeakers), which generates a destructive interference field [10] [15].

When the frequency of a sinusoidal disturbance is known, the *internal model principle* (IMP) [11] can be applied, and consists in incorporating a model of the dynamics of the disturbance signal in the compensator. For a sinusoidal disturbance with constant frequency, this means that the controller should have a pair of poles on the $j\omega$-axis in the s-plane at a location corresponding to the frequency of the disturbance. The *repetitive controller* [25] may be viewed as a special case of IMP controller. The compensator has an infinite number of poles at $\pm j\omega_d$, $\pm j2\omega_d$, $\cdots$ (or $e^{\pm j\omega_d}$, $e^{\pm j2\omega_d}$, $\cdots$ in discrete-time). *Adaptive feedforward cancellation* (AFC) [7] may also be employed and consists in adding the negative of the disturbance's value at the plant input. Adaptation is used to compensate for the unknown magnitude and phase of the disturbance. AFC can also be used if the frequency is unknown, as long as a so-called reference signal is available. In active noise and vibration control, a reference signal is a measurement of the disturbance signal ahead of its point of entry in the system (*i.e.,* an indirect measurement of the disturbance with a shorter time delay than the one associated with the plant).

The frequency of the periodic disturbance is not always known and obtaining a reference signal may not be feasible, or it may be undesirable for reliability or cost considerations. Without a known frequency or a feedforward sensor, the control problem becomes more complicated. An intuitive approach to reject a sinusoidal disturbance with unknown frequency is to construct a frequency estimator and to use the estimated frequency in a disturbance cancellation scheme for known frequency. This concept was called the *indirect approach* in [7] [28]. An advantage of the indirect approach is that the frequency estimator and the disturbance cancellation scheme for known frequency can be designed separately.

In contrast, the *direct approach* attempts to design a stable adaptive controller for rejecting unknown disturbances in an integrated algorithm. A direct approach based on a *magnitude phase-*

locked loop (MPLL) concept can be found in [5] [6] [7], where the estimates of the frequency, phase and magnitude of the periodic disturbance at the input of the plant are incorporated in a single, stable compensator. Periodic disturbance rejection may also be achieved using a direct approach based on the adaptation of an IMP controller [9] [20] [21]. The number of adaptive parameters can be kept small by considering the Youla-Kucera parametrization of the controller (known as the Q-parameterization) [1] [2] [3] [16]. The internal model is adjusted directly in the controller by updating the parameters of the operator Q, and the number of the adaptive parameters of Q is equal to twice the number of sinusoidal components. However, an accurate estimate of the plant transfer function must be available for the implementation of the controller.

This paper focuses on a direct approach for the rejection of disturbances with multiple independent sinusoidal signals. An example of a disturbance rejection problem with two periodic disturbances is the web transport application of [29]. Experiments on a paper machine showed that the spectrum of the tension had large disturbance components at the frequencies of rotation of the winding and unwinding rolls and their second harmonics. The literature also gives examples of estimation of signals with independent but close frequencies, a problem closely related to the control problem considered in this paper. The paper [30] describes the problem of pitch tracking for automatic music transcription. When multiple notes are played together (polyphonic case), the algorithm must track more than one sinusoidal component. Similarly, [18] describe a smart sensor that requires the extraction of a signal from a measured signal containing an additive sinusoidal noise at a separate but close frequency.

The starting point of this paper is the continuous-time adaptive algorithm of [27] for rejecting periodic disturbances with multiple harmonics. The algorithm has a parallel structure, where several copies of a basic algorithm for sinusoidal disturbance rejection are combined to reject an arbitrary periodic disturbance. In [27], it was assumed that the frequencies of the components were harmonically related. This property yielded a design where all the components contributed to the estimation of the fundamental frequency, while at the same time avoiding the problem of two frequency estimates converging to a same value. Here, the frequencies of the sinusoidal components are allowed to be independent and it is shown that a frequency separation block can be used to avoid convergence of two estimates to the same value. Overall, the contributions of this paper are

to:

- convert the MPLL algorithm of [27] to discrete-time, making implementation in practical applications more straightforward;
- present a stability proof using averaging theory [4] [23], thereby justifying the approximations on which the design of the system is based;
- modify the algorithm to enable the tracking of periodic disturbances containing two or more sinusoidal components that are not harmonically related.

Advantages of the MPLL disturbance compensator are its relative simplicity and the ability to design easily a system with pre-specified closed-loop dynamics. Another useful feature of the algorithm is that the disturbance compensator does not require the transfer function of the system to be known in pure disturbance rejection applications. Instead, the frequency response is used, which can be measured directly in a preliminary tuning phase. This feature is advantageous in high-order systems with complicated dynamics and significant delay, such as found in active noise control.

The paper is organized as follows. Section 2 gives the discrete-time adaptive algorithm for a sinusoidal disturbance. The averaging analysis is provided in Section 3. In Section 4, the algorithm is modified to manage disturbances with multiple sinusoidal components. Simulation results demonstrate the benefit of the modification. Active noise control experiments in section 5 show that the algorithm is effective in reducing the error caused by the disturbance for both fixed and slowly time-varying frequencies.

2 Adaptive Algorithm for Single Sinusoid

For simplicity of presentation, we first consider disturbances having a single sinusoidal component. The discrete-time adaptive scheme is shown in Fig. 1. The plant is described as

$$y(z) = P(z)(u_c(z) + u_d(z) - d(z))$$

where $P(z)$ is the plant transfer function, $u_c(z)$, $u_d(z)$ and $d(z)$ are the z-transforms of the stabilizing controller signal, of the disturbance compensation signal, and of the disturbance signal, respectively. The disturbance is assumed to act at the input of the plant and to be of the form

$$d(k) = m_d \cos(\alpha_d(k))$$

with a frequency

$$\omega_d = \alpha_d(k) - \alpha_d(k-1)$$

$C_1(z)$ called the stabilizing controller and is designed to make the closed-loop system stable. $C_2(z)$ is the reference shaping controller, and is used to improve the tracking of the reference input $r(k)$. The compensator $C_3(z)$ is given by

$$C_3(z) = -\frac{C_2(z)}{1 + C_1(z)P(z)}$$

and is used to construct an error signal $\bar{e}$ that is indicative of the error caused by the disturbance without being affected by the reference input. Indeed,

$$\bar{e}(k) = H(z)\left[d(k) - u_d(k)\right] \tag{1}$$

where $H(z)$ is defined as

$$H(z) = \frac{P(z)}{1 + C_1(z)P(z)} \tag{2}$$

and the notation $H(z)\left[(\cdot)\right]$ is used to represent the time-domain output of the discrete-time LTI system $H(z)$ with input $(\cdot)$.

The disturbance compensation signal has the form

$$u_d(k) = m(k)\cos(\alpha(k)) \tag{3}$$

where m is the estimate of the magnitude of the disturbance m_d and α is the estimate of the phase

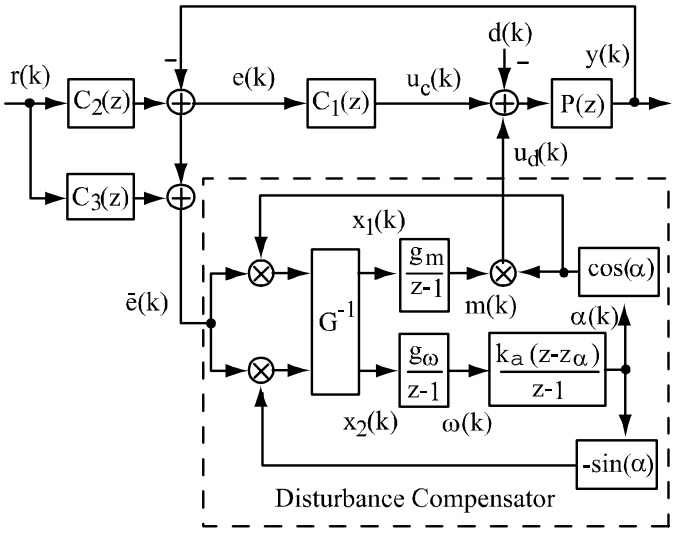

Figure 1: Discrete-time algorithm for rejecting disturbances having a single sinusoidal component

α_d. Similarly, we will denote ω as the estimate of ω_d. The equations of the algorithm in Fig. 1 are

$$\begin{bmatrix} x_1 \\ x_2 \end{bmatrix} = G^{-1} \begin{bmatrix} \bar{e}(k)\cos(\alpha(k)) \\ -\bar{e}(k)\sin(\alpha(k)) \end{bmatrix} \tag{4}$$

where G is a 2×2 matrix

$$G = \frac{1}{2} \begin{bmatrix} H_R(\omega_d) & -H_I(\omega_d) \\ H_I(\omega_d) & H_R(\omega_d) \end{bmatrix} \tag{5}$$

and H_R and H_I are the real and imaginary parts of the frequency response of the system $H(z)$, evaluated at the nominal frequency ω_d

$$\begin{aligned} H_R(\omega_d) &= \mathrm{Re}[H(e^{j\omega_d})] \\ H_I(\omega_d) &= \mathrm{Im}[H(e^{j\omega_d})] \end{aligned} \tag{6}$$

In the implementation of the algorithm, ω_d is replaced by a rough estimate provided a priori, or by the estimate ω.

The remaining signals are given in the z-domain by

$$\begin{aligned} m(z) &= \frac{g_m}{z-1}x_1(z) \\ \omega(z) &= \frac{g_\omega}{z-1}x_2(z) \\ \alpha(z) &= \frac{k_\alpha(z-z_\alpha)}{z-1}\omega(z) \end{aligned} \tag{7}$$

The parameter k_α is chosen so that, for a constant frequency estimate ω, the phase α is the integral of the frequency. Thus,

$$k_\alpha = \frac{1}{1-z_\alpha} \tag{8}$$

It should be noted that the algorithm can be viewed as two separate parts. If $d(k)$ and $u_d(k)$ are not considered, the remaining blocks $P(z)$, $C_1(z)$ and $C_2(z)$ form a standard control system with two degrees of freedom. The subsystem will be called the *nominal closed-loop subsystem*. The system from $\bar{e}(k)$ to $u_d(k)$ can be looked at as an add-on that will be called the *disturbance compensator*. In general, the nominal closed-loop subsystem is designed to achieve stability, tracking of reference inputs, and rejection of broadband noise. Its design should take into account the usual constraints imposed by unmodelled dynamics and measurement noise. The disturbance compensator is added to improve the rejection of residual sinusoidal disturbances of unknown and time-varying frequencies. While the linear time-invariant compensator of the nominal subsystem is unable to completely reject a disturbance with unknown frequency, the disturbance compensator is able to do so asymptotically, at least in the ideal case where there is no measurement noise.

In pure disturbance rejection applications where the reference input is zero (such as active noise control), the transfer functions $C_2(z)$ and $C_3(z)$ can be set to zero and the signal used by the disturbance compensator is $\bar{e} = -y$. A useful feature of the algorithm in this case is that the disturbance compensator does not require the knowledge of the transfer function of the nominal system. Instead, the frequency response is used, and it can be obtained reliably in a preliminary sine sweep experiment (from u_d to y). Model matching to some transfer function is not needed: the raw data can be used directly. This feature is advantageous for high-order systems with complicated dynamics and significant delay, such as found in active noise control. In contrast, algorithms found

in [1], [16] require an estimate of the transfer function of the system in the implementation, resulting in greater computational load and unmodelled dynamics.

In previous work [6] [13] [14], the analysis of schemes similar to the one presented here was performed using approximations that are typically found in the analysis of phase-locked loops. Here, we show that the arguments can be made rigorous by setting the system appropriately in the context of averaging theory (see [4] for the discrete-time theory, or [23] for the continuous-time equivalence).

3 Averaging Analysis

3.1 Background

Of interest here is the discrete-time averaging method for mixed time scale systems [4], which are described by difference equations of the form

$$\begin{aligned} x(k+1) &= x(k) + \epsilon f(k, x(k), y(k), \epsilon) && (9) \\ y(k+1) &= A(x(k))y(k) + h(k, x(k)) \\ &\quad + \epsilon g(k, x(k), y(k), \epsilon) && (10) \end{aligned}$$

The theory relates the solutions of system (9)-(10) to those of the so-called *averaged system*

$$x_{av}(k+1) = x_{av}(k) + \epsilon f_{av}(x_{av}(k)) \tag{11}$$

where

$$f_{av}(x) = \lim_{T \to \infty} \frac{1}{T} \sum_{k=k_0+1}^{k_0+T} f(k, x, w(k, x), 0) \tag{12}$$

and

$$w(k, x) = \sum_{i=0}^{k-1} A(x)^{k-i-1} h(i, x)$$

Assuming that the limit in (12) exists uniformly with respect to k_0 and assuming that the parameter ϵ is sufficiently small, the theory provides that the subset $x(k)$ of the solutions of the nonautonomous

original system (9)-(10) can be approximated by those of the simpler autonomous *averaged system* (11). In particular, if $x = 0$, $y = 0$ and $x_{av} = 0$ are equilibrium states of the two systems, exponential stability of the original system can be inferred from exponential stability of the averaged system.

3.2 Error Formulation and Averaged System

It is not immediately obvious that the adaptive algorithm presented earlier fits into the averaging theory. First, a small parameter ϵ must be artificially introduced in the equations to enable the approximation. Then, proper changes of variables must be applied so that the origin is an equilibrium point of the system and so that stability can be assessed. It turns out that the results can be achieved by the following coordinate change

$$\begin{aligned} \tilde{m}(k) &= m(k) - m_d(k) \\ \epsilon\tilde{\omega}(k) &= \omega(k) - \omega_d \\ \tilde{\alpha}(k) &= \alpha(k) - \alpha_d(k) \end{aligned} \tag{13}$$

and the following redefinition of the adaptation parameters

$$g_m = \epsilon\bar{g}_m,\ g_\omega = \epsilon^2\bar{g}_\omega,\ k_\alpha = \frac{\bar{k}_\alpha}{\epsilon} \tag{14}$$

where ϵ is a "small" scalar parameter. Note that, instead of a standard error formulation $\tilde{\omega}(k) = \omega(k) - \omega_d$, a special error formulation $\epsilon\tilde{\omega}(k) = \omega(k) - \omega_d$ is used, because it turns out that the system with the standard error formation $\tilde{\omega}(k)$ *does not* fit the averaging theory. With these definitions, (7) transforms into

$$\begin{aligned} \tilde{m}(k+1) &= \tilde{m}(k) + \epsilon\left[\bar{g}_m x_1(k)\right] \\ \tilde{\omega}(k+1) &= \tilde{\omega}(k) + \epsilon\left[\bar{g}_\omega x_2(k)\right] \\ \tilde{\alpha}(k+1) &= \tilde{\alpha}(k) + \epsilon\left[\tilde{\omega}(k) + \bar{g}_\omega \bar{k}_\alpha x_2(k)\right] \end{aligned} \tag{15}$$

where $x_1(k)$ and $x_2(k)$ were defined in (4) and can be reformulated as

$$\begin{bmatrix} x_1(k) \\ x_2(k) \end{bmatrix} = G^{-1}\bar{e}(k) \begin{bmatrix} \cos(\tilde{\alpha}(k) + \alpha_d(k)) \\ -\sin(\tilde{\alpha}(k) + \alpha_d(k)) \end{bmatrix} \tag{16}$$

If the closed-loop subsystem $H(z)$ in (2) has a state-space realization

$$\begin{aligned} \theta(k+1) &= A\theta(k) + Bu(k) \\ \bar{e}(k) &= C\theta(k) + Du(k) \end{aligned}$$

with constant matrices $A \in R^{n\times n}$, $B \in R^{n\times 1}$, $C \in R^{1\times n}$, $D \in R^{1\times 1}$ and input $u(k) = d(k) - u_d(k)$, we obtain

$$\begin{aligned} \theta(k+1) &= A\theta(k) + B(m_d \cos(\alpha_d(k)) \\ &\quad -(m_d + \tilde{m}(k)) \cos(\tilde{\alpha}(k) + \alpha_d(k)) \qquad (17) \\ \bar{e}(k) &= C\theta(k) + D(m_d \cos(\alpha_d(k)) \\ &\quad -(m_d + \tilde{m}(k)) \cos(\tilde{\alpha}(k) + \alpha_d(k)) \qquad (18) \end{aligned}$$

Then, (15) and (17) constitute a mixed time scale system, with $x_1(k)$ and $x_2(k)$ obtained by arithmetic computation of (16) and (18).

It remains to determine whether the averaged system is well-defined (i.e., whether the limit in (12) exists. However, note that all the dependencies on time in the mixed time scale system are due to sinusoidal functions and the systems to which they are applied are linear time-invariant systems when the parameters are frozen. As a result, the function f in (12) is periodic, and its average is

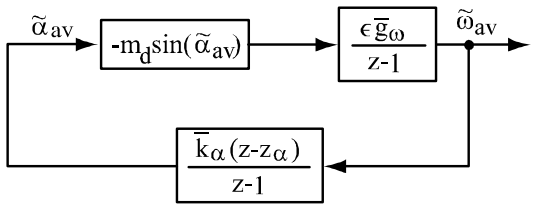

Figure 2: Block diagram of the averaged subsystem — approximate frequency loop

well-defined. In Appendix A, it is shown that the averaged system of (15) and (17) is given by

$$\begin{aligned}
\tilde{m}_{av}(k+1) &= \tilde{m}_{av}(k) - \epsilon \bar{g}_m (\tilde{m}_{av}(k) - \\
&\quad \epsilon \bar{g}_m (m_d - m_d \cos(\tilde{\alpha}_{av}(k))) \\
\tilde{\omega}_{av}(k+1) &= \tilde{\omega}_{av}(k) - \epsilon \bar{g}_\omega m_d \sin(\tilde{\alpha}_{av}(k)) \\
\tilde{\alpha}_{av}(k+1) &= \tilde{\alpha}_{av}(k) + \epsilon \tilde{\omega}_{av}(k) - \\
&\quad \epsilon \bar{g}_\omega \bar{k}_\alpha m_d \sin(\tilde{\alpha}_{av}(k))
\end{aligned} \tag{19}$$

Note that the adaptation of $\tilde{\omega}_{av}$ and $\tilde{\alpha}_{av}$ is not dependent on $\tilde{m}_{av}$. However, the adaptation of $\tilde{m}_{av}$ depends on $\tilde{\alpha}_{av}$, which makes $\tilde{m}_{av}$ track the signal $m_d(\cos(\tilde{\alpha}_{av}) - 1)$. The diagram of the averaged subsystem for $\tilde{\omega}_{av}$ and $\tilde{\alpha}_{av}$ is shown in Fig. 2 and is called the approximate frequency loop. If we returned the system to the original coordinates, we would obtain the nonlinear approximation that was used in [6], but without the supporting theory presented here. It is easy to verify that the averaged system has an equilibrium point at the origin and that the linearized system around the origin is given by

$$\begin{aligned}
\tilde{m}_{av}(k+1) &= \tilde{m}_{av}(k) - \epsilon \bar{g}_m \tilde{m}_{av}(k) \\
\tilde{\omega}_{av}(k+1) &= \tilde{\omega}_{av}(k) - \epsilon \bar{g}_\omega m_d \tilde{\alpha}_{av}(k) \\
\tilde{\alpha}_{av}(k+1) &= \tilde{\alpha}_{av}(k) + \epsilon \tilde{\omega}_{av}(k) - \\
&\quad \epsilon \bar{g}_\omega \bar{k}_\alpha m_d \tilde{\alpha}_{av}(k)
\end{aligned} \tag{20}$$

It will be shown later that this system can be made exponentially stable by proper choice of the adaptation parameters.

3.3 Application of Averaging Theory

Let $x(k)$ denote $\begin{pmatrix} \tilde{m}(k) & \tilde{\omega}(k) & \tilde{\alpha}(k) \end{pmatrix}^T$ and $x_{av}(k)$ be $\begin{pmatrix} \tilde{m}_{av}(k) & \tilde{\omega}_{av}(k) & \tilde{\alpha}_{av}(k) \end{pmatrix}^T$. For some $h > 0$, $\epsilon_0 > 0$, $0 < \epsilon \leq \epsilon_0$, $k \in Z^+$,$T \in Z^+$, assume that:

A1) the closed-loop system $H(z)$ in (2) is stable, which can be obtained by suitably designing $C_1(z)$.

A2) $H_R(\omega)$ and $H_I(\omega)$ are continuous and Lipschitz in ω, where $H_R(\omega)$ and $H_I(\omega)$ are the real and imaginary parts of the frequency response of the system $H(z)$, evaluated at frequency ω.

A3) The initial conditions x_0 and $\tilde{\theta}_0$ (where $\tilde{\theta}$ is defined in (24) in Appendix I) are small enough that $x_{av} \in B_{h'}$ for some $h' < h$ and on the time interval $[0,\ \text{fix}(T/\epsilon)]$ (where $\text{fix}(T/\epsilon)$ denotes the largest integer l such that $l \leq T/\epsilon$).

Then, the following lemmas can be derived from [4] after verification of assumptions $B1 - B7$ of the paper(see Appendix B).

Lemma 1: (Basic Averaging Lemma):

Consider the mixed time scale system (15), (17) and the averaged system (19) with assumptions $A1$ and $A2$. Then, there is an ϵ_T, $0 < \epsilon_T \leq \epsilon_0$ and a class K function $\Psi(\epsilon)$ such that

$$\|x(k) - x_{av}(k)\| \leq \Psi(\epsilon) b_T$$

for some $b_T > 0$ and for all $k \in [0,\ \text{fix}(T/\epsilon)]$ and $0 < \epsilon \leq \epsilon_T$.

Lemma 2. (Exponential Stability Lemma)

If the original system in (15) and the averaged system in (19) satisfy assumptions $A1 - A3$, and if the averaged system is locally exponentially stable, the equilibrium point $x = 0$ of the original system is locally exponentially stable for $m_d \neq 0$ and ϵ sufficiently small.

To illustrate the validity of the averaging analysis, we consider an example with identity plant $P(z) = 1$ and $C_1(z)$, $C_2(z)$, $C_3(z)$ are all zero. No reference input signal is applied and the disturbance is chosen as $d(k) = \cos(0.2k\pi + 0.2\pi)$. Parameters and initial conditions for the averaged system in (19) are $\bar{g}_m = 0.5$, $\bar{g}_\omega = 1$, $\bar{k}_\alpha = 2$, $\tilde{m}(0) = 0.1$, $\tilde{\omega}(0) = 0.1\pi$, $\tilde{\alpha}(k) = -0.2\pi$. The

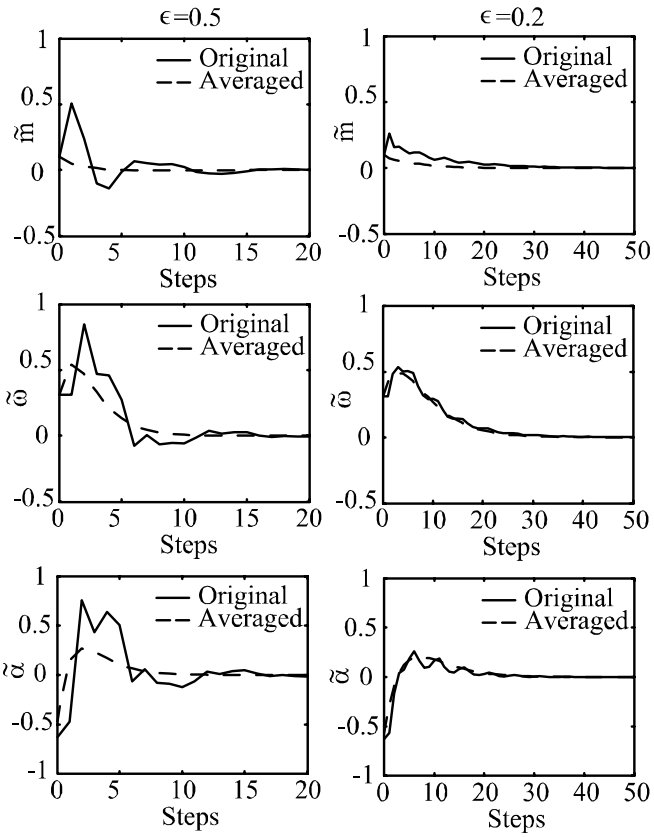

Figure 3: Parameter errors for both the original and averaged systems: with larger ϵ (left) and with smaller ϵ (right)

simulation parameters of the original system are transformed back by (13) and (14). Fig. 3 shows the plots of the parameter errors $\tilde{m}$, $\tilde{\omega}$ and $\tilde{\alpha}$ for both the original and averaged systems, with two different adaptation gains having $\epsilon = 0.5$ and $\epsilon = 0.2$. It can be seen that the approximation of the averaged system is closer to the original one for smaller ϵ.

Note that the two lemmas are based on the assumption that the initial condition $x_0 \in R^3$ is sufficiently close to zero, and $\tilde{\omega}(0)$ is an element of x_0. Recall from (13) that $\epsilon\tilde{\omega}(0) = \omega(0) - \omega_d$. Thus, the initial frequency estimate $\omega(0)$ must become closer to the nominal frequency ω_d when ϵ tends to zero for the approximation to be valid. Intuitively, this can be explained by the fact that one of the states of the system (the angle of the MPLL) is the integral of another state (the frequency of the MPLL). As the system is slowed down by reducing ϵ , the initial error in the frequency must be reduced to insure that trajectories stay close to the averaged system trajectories.

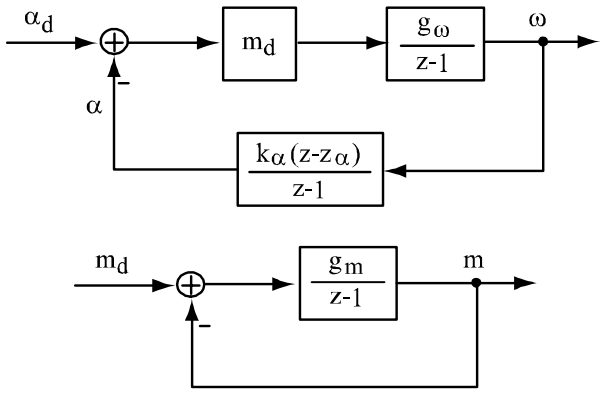

Figure 4: Linear approximation of the frequency loop (top) and magnitude loop (bottom)

3.4 Linear Analysis of the Averaged System and Exponential Stability

The linear approximation of the averaged system (20) gives two decoupled systems which, transformed to the original variables, yield the diagrams in Fig. 4.

For the approximate frequency loop in Fig. 4, the poles of the closed-loop system can be placed by appropriate choice of the controller parameters. Given $z_{d,\omega}$ some desired location in the z plane (inside the unit circle), the following parameters will result in two poles at that location

$$\begin{aligned} g_\omega &= \frac{(1 - z_{d,\omega})^2}{m_d} \\ z_\alpha &= \frac{1 + z_{d,\omega}}{2} \end{aligned} \tag{21}$$

Since m_d is not known, a solution consists in using an upper bound. The approximate frequency loop will have stable poles for all values of m_d less than the upper bound, and the poles will be equal to $z_{d,\omega}$ when m_d is equal to its upper bound.

For the magnitude loop, the closed-loop pole can be placed at $z_{d,m}$ by letting

$$g_m = 1 - z_{d,m} \tag{22}$$

Choosing stable values for the desired poles yields an averaged system that is locally exponentially stable. The theory of averaging can be applied by choosing values of $z_{d,\omega}$ and $z_{d,m}$ that are sufficiently close to 1. However, although the linear approximation may not give precise estimates of the original system when ϵ is small, the approximation is often still indicative of the asymptotic

convergence of the algorithm and it is very useful for design, especially for setting the parameter gains.

To implement the algorithm, initial estimates of the magnitude and the frequency of the disturbance should be used. The estimate of the frequency of the disturbance is needed to adjust G^{-1}, which may then be updated as a function of the estimate ω, or may be kept unchanged during the adaptation if the prior estimate is sufficiently precise. In the case where the initial frequency is far from ω_d, the averaging analysis is not valid anymore, as the averaged out terms (e_1 and e_2 in Appendix A) cannot be overlooked. It may take a longer time for ω to lock to ω_d, due to complex nonlinear dynamics. For a single sinusoidal component, estimates of the lock-in time can be obtained using approximations found in the theory of phase-locked loops [26].

4 Extension to Multiple Components

In this section, it is assumed that the disturbance $d(k)$ contains multiple sinusoidal components, so that

$$\begin{aligned} d(k) &= \sum_{i=1}^{N} m_{d,i} \cos(\alpha_{d,i}(k)) \\ \omega_{d,i} &= \alpha_{d,i}(k+1) - \alpha_{d,i}(k), \quad i = 1, \cdots, N \end{aligned}$$

The number of components N is assumed to be known a priori. If not, methods such as found in [12] and its references can be used to estimate the number of sinusoids. Given that the parameters $m_{d,i}$, $\omega_{d,i}$, $\alpha_{d,i}$ (for $i = 1, \cdots, N$) are unknown, a natural method is to employ several disturbance rejection blocks to eliminate all the components of $d(k)$.

4.1 Algorithm

The proposed algorithm is shown in Fig. 5. Each disturbance compensator is updated by the signal $\bar{e}(k)$, and the outputs of the compensators are summed up to cancel the effect of $d(k)$. The i^{th} compensator is a copy of the algorithm in Fig. 1, with an additional subscript i (for $i = 1, \cdots, N$) associated to the specific component. If the MPLL algorithm is copied N times as the disturbance

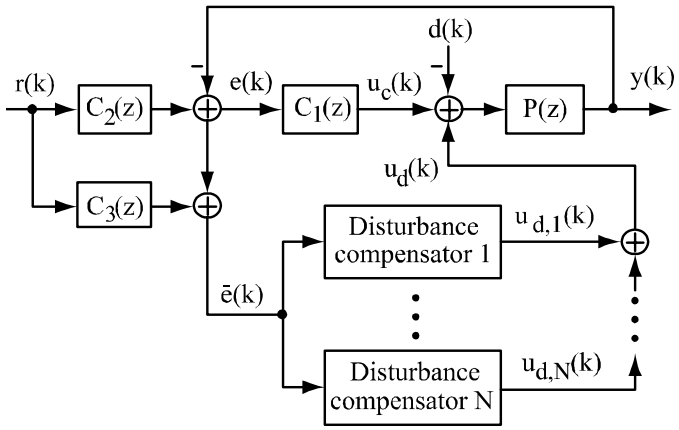

Figure 5: Adaptive scheme for disturbances with multiple sinusoidal components

compensator, it turns out that the averaged system of Fig. 5 becomes a collection of independent, averaged systems for single sinusoid as in (19) because product terms originating from distinct frequencies average out to zero. Similar design techniques can therefore be used for the individual compensators. Although not common, it is possible for two frequency estimates to converge to the same value. We propose here a technique that has been found useful to avoid this problem.

4.2 Frequency Separation

The update of ω_i is

$$\omega_i(k+1) = \omega_i(k) + g_{\omega,i} x_{2,i}(k) \tag{23}$$

except when some estimated frequencies become too close. Then, a separation component is used to prevent any two estimators from converging to the same frequency (such problem was found to occur in simulations, although infrequently).

The proposed *separation scheme* is designed as follows. Given a minimum frequency separation Δ, a small parameter set by the designer:

1) $\hat{\omega}_i(k+1) = \omega_i(k) + g_{\omega,i} x_{2,i}(k)$.

2) Let $\hat{\omega}_m = \frac{1}{N} \sum_{i=1}^{N} \hat{\omega}_i(k+1)$ and sort $\hat{\omega}_i(k+1)$ in *descending* order. Then, label the sorted elements as $\bar{\omega}_i$ and the corresponding index as $s(i)$, meaning that $\bar{\omega}_i = \hat{\omega}_{s(i)}(k+1)$ and $\bar{\omega}_i \geq \bar{\omega}_{i+1}$ for all i. Find the (largest) index j such that $\bar{\omega}_j \geq \hat{\omega}_m > \bar{\omega}_{j+1}$.

3) Let $\delta = \bar{\omega}_j - \bar{\omega}_{j+1}$

- If $\delta < \Delta$, then $\bar{\omega}_j = \bar{\omega}_j + \frac{\Delta - \delta}{2}$ and $\bar{\omega}_{j+1} = \bar{\omega}_{j+1} - \frac{\Delta - \delta}{2}$
- Else, keep $\bar{\omega}_j$ and $\bar{\omega}_{j+1}$ unchanged.

4) For $i = j - 1, \cdots, 1$, let $\delta = \bar{\omega}_i - \bar{\omega}_{i+1}$

- If $\delta < \Delta$, then $\bar{\omega}_i = \bar{\omega}_{i+1} + \Delta$
- Else, continue.

5) For $i = j + 2, \cdots, N$, let $\delta = \bar{\omega}_{i-1} - \bar{\omega}_i$

- If $\delta < \Delta$, then $\bar{\omega}_i = \bar{\omega}_{i-1} - \Delta$
- Else, continue.

6) Assign the modified sorted frequency $\bar{\omega}_i$ to the corresponding frequency estimates $\omega_{s(i)}(k+1)$ based on the order obtained in step 2.

It should be noted that, in step 1, it is theoretically possible that several $\hat{\omega}_i$'s have equal value. This is not a problem, but it may be preferable to select the indices in step 2 to preserve the original ordering in such case.

The separation scheme has the following properties:

- $|\omega_i - \omega_j| \geq \Delta$ for all $i \neq j$ (*i.e.,* the frequency estimates are all separated by an amount greater than or equal to Δ).
- $|\omega_i - \hat{\omega}_i| \leq (N-1) \cdot \Delta$ for all i (*i.e.,* the frequency estimates are only modified by small amounts if Δ is small).
- if $|\hat{\omega}_i - \hat{\omega}_j| \geq \Delta$ for all i, j and $i \neq j$, then $\omega_i = \hat{\omega}_i$ for all i (*i.e.,* the frequency estimates are not modified if they are already sufficiently separated).

Although the frequency separation is helpful to avoid the problem of two estimates converging to the same value, it is generally desirable to have reasonably good prior estimates of the frequencies. If such estimates are not available, a solution consists in applying some of the eigenvector-based

methods available in the signal processing literature [19] [24]. The *multiple signal classification* (MUSIC) frequency estimation method and the *estimation of signal parameters via rotational invariance techniques* (ESPRIT) algorithm are two such methods that can be used to obtain estimates of the frequency values before engaging the adaptive algorithm. However, the following simulations and experiments show the ability of the MPLL algorithm to acquire and track time-varying frequencies even with large initial frequency errors.

4.3 Simulation Results

In this section, we consider a simulation with a plant

$$P(z) = \frac{z}{z - 1.1}$$

and controllers $C_1(z)$ and $C_2(z)$ chosen as

$$\begin{aligned} C_1(z) &= \frac{0.749(z - 0.9)}{z - 1} \\ C_2(z) &= \frac{0.05}{z - 0.95} \end{aligned}$$

so that both poles of the nominal closed-loop subsystem are located at 0.79, and the step response from $r(k)$ to $y(k)$ has no overshoot. The reference input $r(k)$ is 0 for the first 1500 steps and is 1 for the next 1500 steps. The disturbance $d(k)$ has two sinusoidal components with nominal parameters $m_{d,1} = 1$, $m_{d,2} = 0.3$, $\omega_{d,1} = 0.01 \times 2\pi$, $\omega_{d,2} = 0.02 \times 2\pi$, $\alpha_{d,1}(0) = 0$, $\alpha_{d,2}(0) = 3\pi/2$. The initial values of the estimates of the disturbance compensators $m_1 = 1.2$, $m_2 = 0.5$, $\omega_1 = 0.007 \times 2\pi$, $\omega_2 = 0.014 \times 2\pi$, and 0 for the phases. The desired closed-loop poles for the disturbance compensators are selected as $z_{d,\omega,1} = 0.98$, $z_{d,\omega,2} = 0.987$, and $z_{d,m,i} = 0.995$ for $i = 1$ and 2. This leads to parameters of the algorithm $g_{m,1} = g_{m,2} = 0.01$, $g_{\omega,1} = 4 \times 10^{-4}$, $g_{\omega,2} = 5.633 \times 10^{-4}$, $z_{\alpha,1} = 0.99$, $z_{\alpha,2} = 0.9935$, $k_{\alpha,1} = 100$, $k_{\alpha,2} = 153.85$. In the simulations, these parameters were kept fixed and the matrix G^{-1} was updated with the frequency estimate ω, assuming that the plant was known exactly.

Fig. 6 gives the plant output without disturbance compensation. Fig. 7 shows the output

of the plant $y(k)$ with and without frequency separation scheme. The parameter Δ used in the separation scheme was $0.002 \times 2\pi$. The plot on the top shows the plant output when there is no separation component. A large residual error is apparent. This can be explained by Fig. 8 (top plot) which shows the two frequency estimates converging to the same value around $0.01 \times 2\pi$, and leaving the other disturbance component uncompensated for. The bottom plots of the two figures, obtained with the *separation scheme*, show that the effect of the disturbance is eliminated and that the frequency estimates converge to the correct values. They also show that the adaptive system converges in 1000 steps (10 periods for $\omega_{d,1}$).

The time of convergence is somewhat slow compared to what can be achieved with a single sinusoidal component. Conditions were deliberately chosen to be challenging, with relatively large initial frequency errors (30% off the nominal ones) and close disturbance frequencies. In frequency estimation, one finds that the discrimination of two close frequencies involves time constants associated to the difference in the frequencies, instead of the frequencies themselves. Also, [8] reports the need to decrease the convergence speed of another adaptive control algorithm in similar experimental conditions.

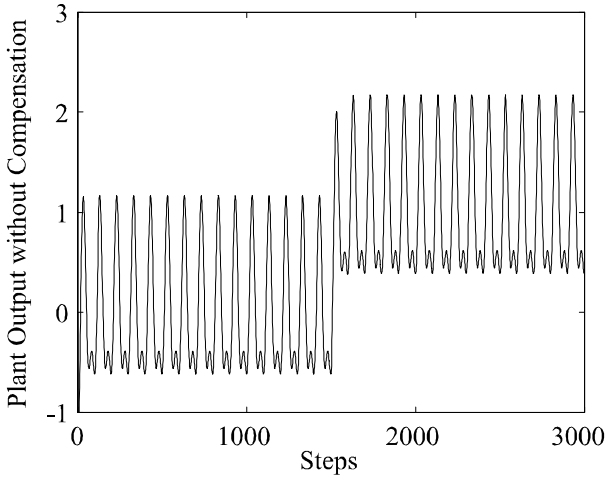

Figure 6: Plant output without any disturbance compensators

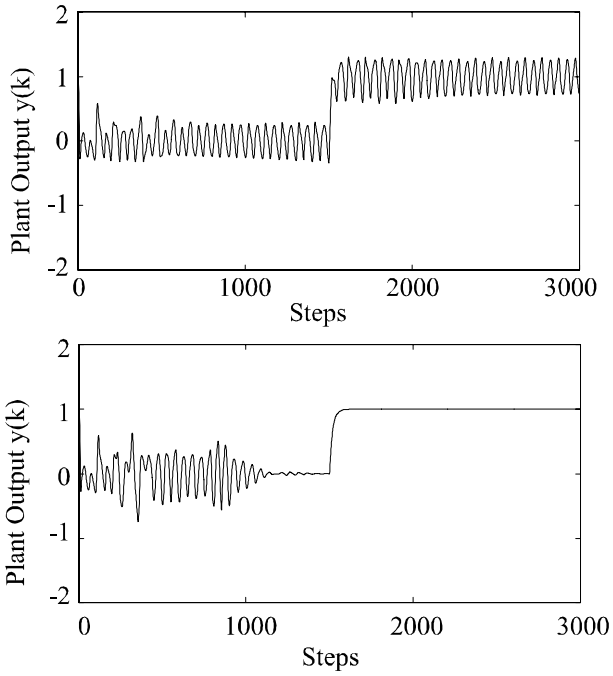

Figure 7: Plant output: disturbance rejection algorithm without separation (top) and with separation scheme 1 (bottom)

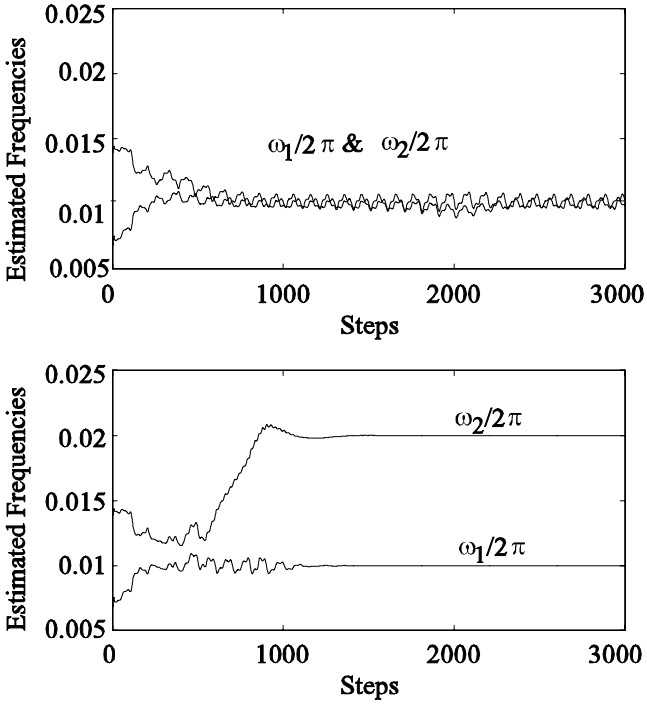

Figure 8: Frequency estimates: without separation (top) and with separation scheme 1 (bottom)

5 Active Noise Control Experiments

5.1 Experimental Set-up

The adaptive algorithm for the rejection of periodic disturbances with multiple sinusoidal components was implemented on an active noise control system developed at the University of Utah. The

algorithm was coded in C language and downloaded in a dSPACE DS1104 controller board hosted in a PC. The sampling rate was 8 kHz. The adaptive algorithm requires knowledge of the frequency response of the plant. The characteristics of $P(e^{j\omega})$ are unknown but can be estimated in a training stage. After the training, the estimated model $\hat{P}(e^{j\omega})$ is used in the algorithm for the experiments. The frequency response at a given frequency ω_0 was estimated by an *empirical transfer function estimate* (ETFE [17]) method, where the plant input was a pure sinusoid $cos(\omega_0 k)$. The real and imaginary parts of the frequency response were obtained at 91 frequencies, equally spaced between 50 Hz and 500 Hz, and the results were saved in a look-up table. The range was found appropriate for active noise control [15]. In real-time application, the real and imaginary parts of the frequency response at the estimated frequency were obtained by linearly interpolating the look-up table, and the matrices G_i $(i = 1 \cdots N)$ were updated based on their respectively estimated frequencies ω_i, which correspond to the continuous-time frequencies $\omega_i/2\pi \times 8000$ (in Hz). In the experiments, all noise sources contained two sinusoidal components and the controllers $C_1(z)$, $C_2(z)$, $C_3(z)$ in Fig. 5 were all set to be zero. As mentioned earlier, the disturbance rejection application does not require knowledge or implementation of the plant transfer function in that case.

5.2 Experiment with Fixed Frequencies

In this experiment, the nominal frequencies were fixed at $0.02 \times 2\pi$ radians/step and $0.05 \times 2\pi$ radians/step, which correspond to 160 *Hz* and 400 *Hz* respectively in continuous-time. The initial frequency estimates were set to be $0.015 \times 2\pi$ and $0.045 \times 2\pi$, and all other parameters were initially set at zero. The algorithm was not engaged until 1 second (corresponding to 8000 steps), so that the effect of the noise before compensation could be evaluated. The desired closed-loop poles were set at $z_{d,\omega,i} = 0.99$ and $z_{d,m,i} = 0.96$, for $i = 1, 2$. The separation procedure was not employed since the estimates were widely separated.

Fig. 9 shows the signal obtained from the error microphone. It shows that the algorithm, once engaged, reduced the noise significantly within 0.3 second. The attenuation of noise is also evaluated in the frequency domain by taking the spectral density of the error microphone before the use of the algorithm (data in the first second of Fig. 9) and after the algorithm has converged (data from the 2^{nd} second to the 5^{th} second). The spectral density of the signals was obtained using Welch's

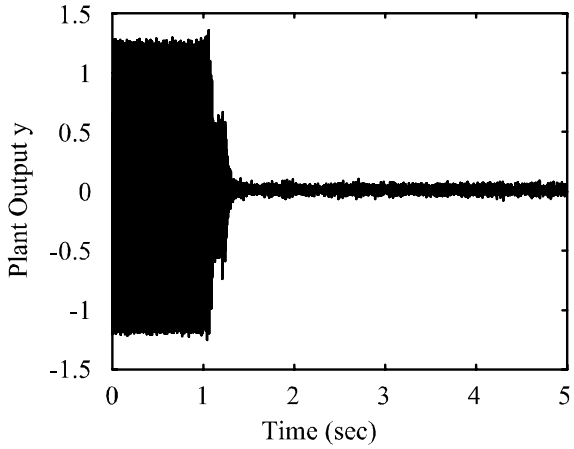

Figure 9: Microphone signal

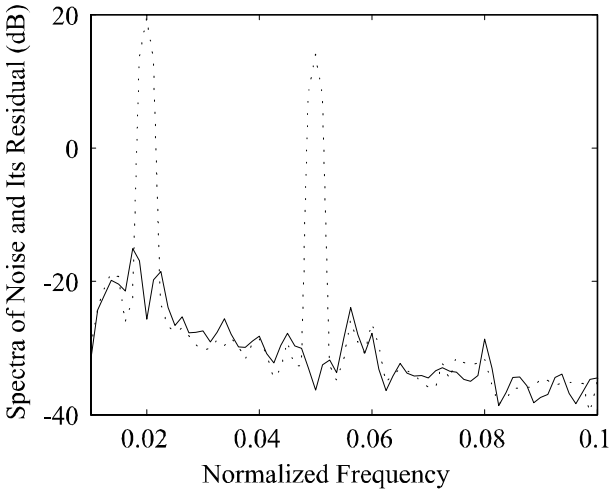

Figure 10: Spectra of microphone signal before algorithm (dotted line) and after convergence (solid line)

averaged periodogram method with nonoverlapping Hanning window having a length of 800 samples (using the function *spectrum.m* in Matlab). Fig. 10 shows the results with normalized frequency from 0.01 to 0.1, where the dotted line (spectral density before algorithm engaged) demonstrates significant spectral contents around normalized frequency 0.02 and 0.05. The solid line shows that the two components are reduced greatly by more than 40dB after the algorithm has converged. The estimated frequencies and magnitudes are also shown in Fig. 11 and Fig. 12.

5.3 Experiment with Varying Frequencies

In this section, the experiment was performed with noise frequencies that changed with time. The first frequency varied linearly between $0.02 \times 2\pi = 0.126$ (160 Hz) and $0.018 \times 2\pi = 0.113$

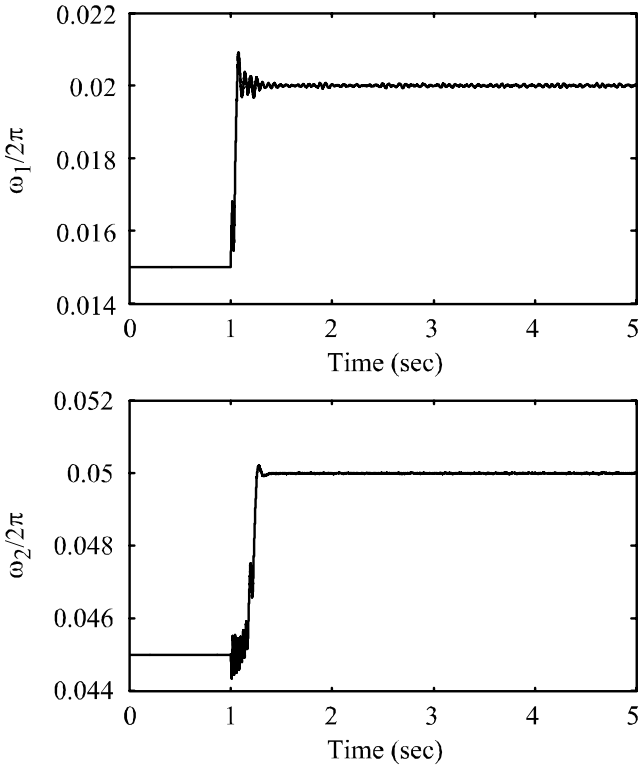

Figure 11: Frequency estimates of the control signal

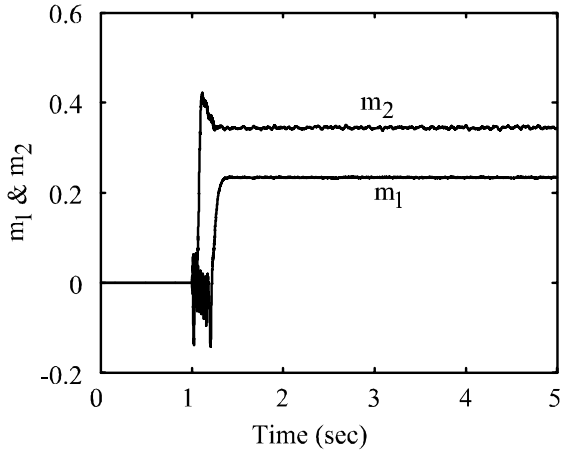

Figure 12: Magnitude estimates of the controller

(144 Hz), and the second frequency changed linearly between $0.05 \times 2\pi = 0.314$ (400 Hz) and $0.048 \times 2\pi = 0.302$ (384 Hz). The initial frequencies were set at the correct frequencies at time 0. Both closed loop poles of the frequency loop were located at $z_{d,\omega} = 0.998$, and the poles of the magnitude loop were set at $z_{d,m} = 0.999$. All other parameters were initially set to zero.

Fig. 13 shows the signal at the microphone without disturbance compensation (top) and the corresponding error signal when the disturbance control signal was applied (bottom). One finds that

the disturbance was reduced dramatically despite the variation of the frequencies. The estimated frequencies and the corresponding estimated frequency errors are shown in Fig. 14 and Fig. 15. Fig. 16 demonstrates that the estimated magnitudes are time-varying, although the noise signal from the D/A has constant magnitudes. This is due to the variation in frequency response of the noise path and of the plant. An example of the plant magnitude response for an active noise control testbed may be found in [27].

Tracking of the frequencies, as shown in Fig. 14 is excellent. Although the rate of variation of the frequencies is slow, it is comparable to the case of noise cancellation in a turboprop aircraft where the rotating blade frequencies are of the order of 100Hz and engine speed variations occur over periods of seconds. If the rate of variation increases, a higher delay will be incurred in the estimates. The controller may need to be redesigned. For example, the delay for ramp inputs can be eliminated by increasing the order and type of the compensator of the frequency loop. A unique feature of this algorithm, however, is that the delay can be predicted from the linear analysis. Therefore, a design can be evaluated knowing quantitatively the trade-off between tracking of frequency variations and immunity to noise. Other algorithms available for this problem do not provide such knowledge.

6 Conclusions

The paper proposed an adaptive algorithm for the rejection of disturbances having multiple sinusoidal components of unknown frequency. Although the scheme is characterized by complex nonlinear dynamics, averaging analysis was applied to obtain a nonlinear approximation of the system and linearization enabled a relatively straightforward linear design of the controller. A separation scheme was proposed to avoid the risk of convergence of the frequency estimates to the same value and was shown to be useful in simulations. ANC experiments showed that the algorithm was effective at rejecting the disturbances both when the frequencies were constant and when they were slowly varying.

Appendix A: Averaged System

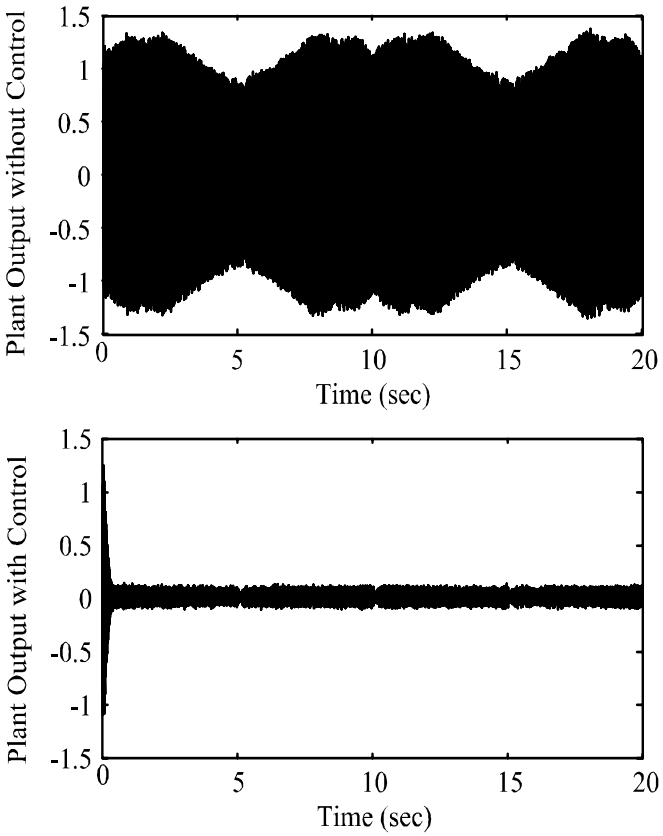

Figure 13: Mirophone signal without (top) and with control (bottom)

Let $x(k)$ denote $\begin{pmatrix} \tilde{m}(k) & \tilde{\omega}(k) & \tilde{\alpha}(k) \end{pmatrix}^T$. By defining the function

$$w(k,x) = \sum_{i=0}^{k-1} A^{k-1-i} B(m_d \cos(\alpha_d(i)) - (m_d + \tilde{m}(i)) \cos(\tilde{\alpha}(i) + \alpha_d(i)))$$

and the transformation

$$\tilde{\theta}(k) = \theta(k) - w(k,x) \tag{24}$$

the error signal $\bar{e}(k)$ in (18) can be expressed as

$$\begin{aligned} \bar{e}(k) &= C(w(k,x) + \tilde{\theta}(k)) + D(m_d \cos(\alpha_d(k)) - (m_d + \tilde{m}(k)) \cos(\tilde{\alpha}(k) + \alpha_d(k))) \\ &= \bar{e}_1(k) - \bar{e}_2(k) + C\tilde{\theta}(k) \end{aligned} \tag{25}$$

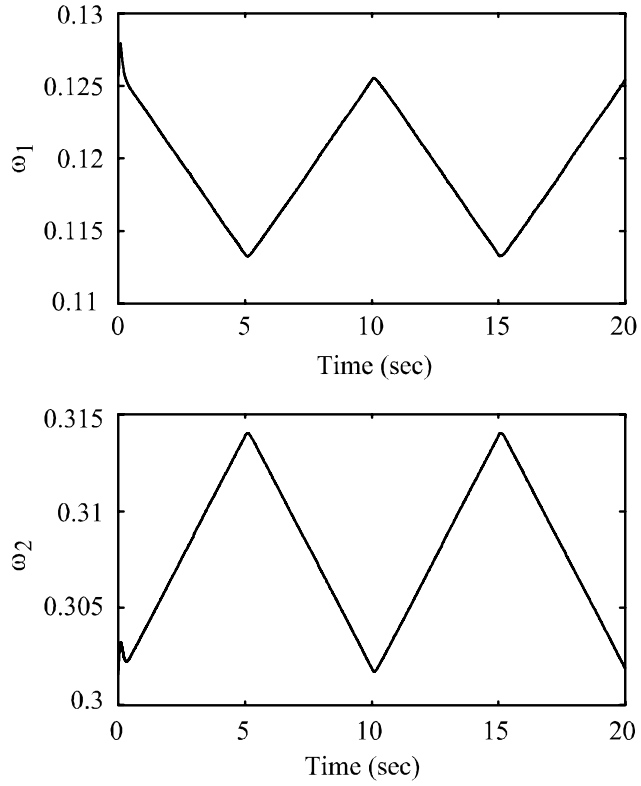

Figure 14: Frequency estimates of the control signal

where

$$\begin{aligned}
\bar{e}_1(k) &= \sum_{i=0}^{k-1} CA^{k-1-i}B(m_d\cos(\alpha_d(i)) + Dm_d\cos(\alpha_d(k)) \\
\bar{e}_2(k) &= \sum_{i=0}^{k-1} CA^{k-1-i}B(m_d+\tilde{m}(i))\cos(\tilde{\alpha}(i)+\alpha_d(i)) + D(m_d+\tilde{m}(k))\cos(\tilde{\alpha}(k)+\alpha_d(k)) \quad (26)
\end{aligned}$$

The signal $\cos(\alpha_d(k))$ has instantaneous frequency ω_d and $\cos(\tilde{\alpha}(k)+\alpha_d(k))$ has instantaneous frequency $\omega_d + \epsilon\tilde{\omega}$.

Both $\bar{e}_1(k)$ and $\bar{e}_2(k)$ are the outputs of a linear system $\Sigma(A,B,C,D)$ with sinusoidal inputs and zero initial conditions. The averaged system is obtained by taking $\tilde{m}$, $\tilde{\alpha}$, $\tilde{\omega}$ to be constants, so that

$$\begin{aligned}
\bar{e}_1(k) &= H_R(\omega_d)m_d\cos(\alpha_d(k)) - H_I(\omega_d)m_d\sin(\alpha_d(k)) + \tilde{e}_1(k) \\
\bar{e}_2(k) &= H_R(\omega_d+\epsilon\tilde{\omega})(\tilde{m}+m_d)\cos(\tilde{\alpha}(k)+\alpha_d(k)) - H_I(\omega_d+\epsilon\tilde{\omega})(\tilde{m}+m_d)\sin(\tilde{\alpha}(k)+\alpha_d(k)) + \tilde{e}_2(k)
\end{aligned}$$

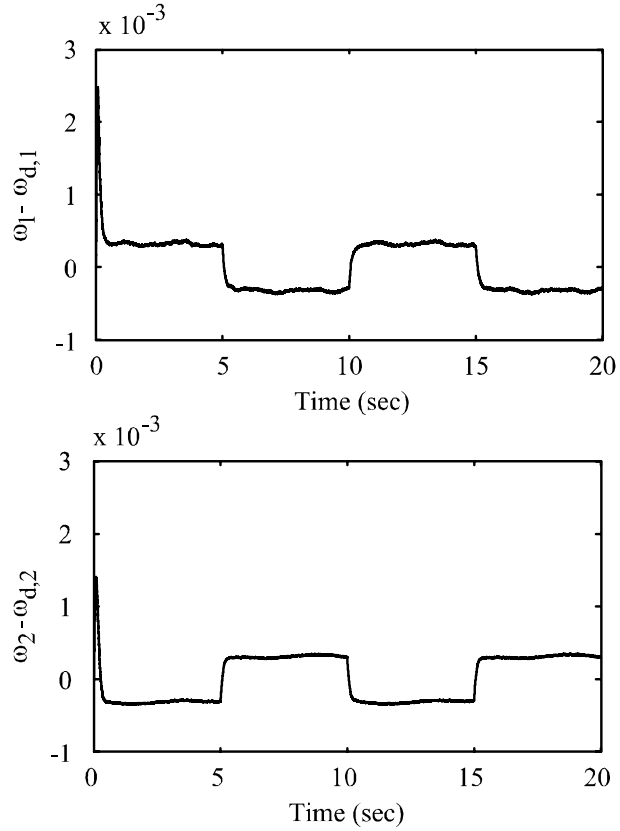

Figure 15: Frequency errors between the estimates and their nominal values

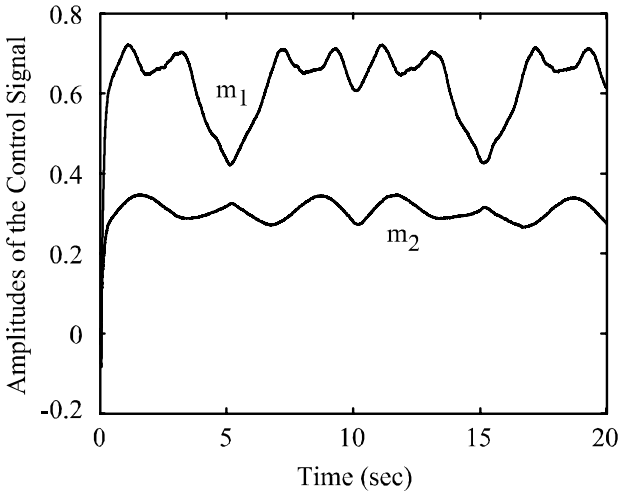

Figure 16: Amplitude estimates of the control signal

where $\tilde{e}_1(k)$ and $\tilde{e}_2(k)$ are transient terms tending to 0 exponentially as $k \to \infty$, given that the closed-loop system is stable.

To lighten the notation, we drop the time index k for all signals. However, the reader should remember that they remain functions of time. Then

$$\bar{e}\begin{pmatrix}\cos(\tilde{\alpha}+\alpha_d)\\ -\sin(\tilde{\alpha}+\alpha_d)\end{pmatrix} = e_1+e_2+e_3$$

where

$$e_1 = \frac{1}{2}\begin{pmatrix} H_R(\omega_d)m_d\cos(\tilde{\alpha}) + H_I(\omega_d)m_d\sin(\tilde{\alpha}) - H_R(\omega_d+\epsilon\tilde{\omega})(\tilde{m}+m_d)\\ -H_R(\omega_d)m_d\sin(\tilde{\alpha}) + H_I(\omega_d)m_d\cos(\tilde{\alpha}) - H_I(\omega_d+\epsilon\tilde{\omega})(\tilde{m}+m_d)\end{pmatrix}$$

$$e_2 = \frac{1}{2}\begin{bmatrix}\gamma_1 & \gamma_2\\ \gamma_2 & -\gamma_1\end{bmatrix}\begin{pmatrix}\cos(2\alpha_d)\\ \sin(2\alpha_d)\end{pmatrix}$$

$$e_3 = (\tilde{e}_1-\tilde{e}_2+C\tilde{\theta})\begin{bmatrix}\cos(\tilde{\alpha}) & -\sin(\tilde{\alpha})\\ -\sin(\tilde{\alpha}) & -\cos(\tilde{\alpha})\end{bmatrix}\begin{pmatrix}\cos(\alpha_d)\\ \sin(\alpha_d)\end{pmatrix}$$

and

$$\begin{aligned}\gamma_1 &= H_R(\omega_d)m_d\cos(\tilde{\alpha}) - H_I(\omega_d)m_d\sin(\tilde{\alpha}) - H_R(\omega_d+\epsilon\tilde{\omega})(\tilde{m}+m_d)\cos(2\tilde{\alpha})\\ &\quad + H_I(\omega_d+\epsilon\tilde{\omega})(\tilde{m}+m_d)\sin(2\tilde{\alpha})\\ r_2 &= -H_R(\omega_d)m_d\sin(\tilde{\alpha}) - H_I(\omega_d)m_d\cos(\tilde{\alpha}) + H_R(\omega_d+\epsilon\tilde{\omega})(\tilde{m}+m_d)\sin(2\tilde{\alpha})\\ &\quad + H_I(\omega_d+\epsilon\tilde{\omega})(\tilde{m}+m_d)\cos(2\tilde{\alpha})\end{aligned}$$

Letting $\epsilon = 0$ and $\tilde{\alpha}$, $\tilde{\omega}$, $\tilde{m}$ be constant, we obtain,

$$AVG\left[e_1\right] = G(\omega_d)\begin{pmatrix}-\tilde{m}_{av}(k) - m_d + m_d\cos(\tilde{\alpha}_{av}(k))\\ -m_d\sin(\tilde{\alpha}_{av}(k))\end{pmatrix}$$

and $AVG\left[e_2\right]=0$, $AVG\left[e_3\right]=0$. It follows that

$$\begin{aligned} AVG\left[\begin{pmatrix} x_1 \\ x_2 \end{pmatrix}\right] &= AVG\left[G^{-1}(\omega_d)\bar{e}\begin{pmatrix} \cos(\alpha) \\ -\sin(\alpha) \end{pmatrix}\right] \\ &= G^{-1}(\omega_d)\times AVG\left[e_1+e_2+e_3\right] \\ &= \begin{pmatrix} -\tilde{m}_{av}(k)-m_d+m_d\cos(\tilde{\alpha}_{av}(k)) \\ -m_d\sin(\tilde{\alpha}_{av}(k)) \end{pmatrix} \end{aligned}$$

Appendix B: Verification of the Assumptions of Averaging Theory

Let

$$\begin{aligned} f(k,x,\tilde{\theta},\epsilon) &= \begin{pmatrix} 0 \\ 0 \\ \tilde{\omega}(k) \end{pmatrix} + \frac{\bar{e}(k)}{H_R^2(\omega_d)+H_I^2(\omega_d)} \\ &\times \begin{pmatrix} \bar{g}_m(H_R(\omega_d)\cos(\tilde{\alpha}(k)+\alpha_d(k))-H_I(\omega_d)\sin(\tilde{\alpha}(k)+\alpha_d(k))) \\ \bar{g}_\omega(-H_I(\omega_d)\cos(\tilde{\alpha}(k)+\alpha_d(k))-H_R(\omega_d)\sin(\tilde{\alpha}(k)+\alpha_d(k))) \\ \bar{g}_\omega\bar{k}_\alpha(-H_I(\omega_d)\cos(\tilde{\alpha}(k)+\alpha_d(k))-H_R(\omega_d)\sin(\tilde{\alpha}(k)+\alpha_d(k))) \end{pmatrix} \end{aligned} \tag{27}$$

$$f_{av}(x)=\begin{pmatrix} -\bar{g}_m(\tilde{m}+m_d-m_d\cos(\tilde{\alpha})) \\ -\bar{g}_\omega m_d\sin(\tilde{\alpha}) \\ \tilde{\omega}-\bar{g}_\omega\bar{k}_\alpha m_d\sin(\tilde{\alpha}) \end{pmatrix}$$

and define $d(k,x)=f(k,x,0,0)-f_{av}(x)$. Given assumption $A2$ of section 3.3 and the facts that

$$\begin{aligned} \|\sin(x_1)-\sin(x_2)\| &\leq \|x_1-x_2\| \\ \|\cos(x_1)-\cos(x_2)\| &\leq \|x_1-x_2\| \\ \|\sin(x_1)\| &\leq 1 \\ \|\cos(x_1)\| &\leq 1 \end{aligned}$$

the following results can be justified for $\forall x\in B_h$, $\forall\tilde{\theta}\in B_h$, $0<\epsilon\leq\epsilon_0$ and $k\in Z^+$:

B1) $x = 0$, $\tilde{\theta} = 0$ is an equilibrium point of (27), i.e., $f(k, 0, 0, \epsilon) = 0$, and $f(k, x, \tilde{\theta}, \epsilon)$ is Lipschitz in x, $\tilde{\theta}$.

B2) $f(k, x, \tilde{\theta}, \epsilon)$ is Lipschitz in ϵ, linearly in x, $\tilde{\theta}$.

B3) $f_{av}(0) = 0$ and $f_{av}(x)$ is Lipschitz in x.

B4) $d(k, x)$ is piecewise continuous in k, has bounded and continuous first derivative in x, and $d(k, 0) = 0$. Moreover, there is a nonnegative strictly decreasing function $\gamma(k)$ with the property $\gamma(k) \to 0$ as $k \to \infty$, so that

$$\left\| \frac{1}{T} \sum_{k=k_0+1}^{k_0+T} d(k, x) \right\| \leq \gamma(T) \|x\|$$

and

$$\left\| \frac{1}{T} \sum_{k=k_0+1}^{k_0+T} \frac{\partial}{\partial x} d(k, x) \right\| \leq \gamma(T)$$

B5) A is uniformly exponential stable, which is known by assumption $A1$ in section 3.3.

B6) Same as assumption $A3$ in section 3.3.

B7) Let $h(k, x) = m_d \cos(\alpha_d(k)) - (m_d + \tilde{m}(k)) \cos(\tilde{\alpha}(k) + \alpha_d(k))$, we can check that $h(k, 0) = 0$, and

$$\left\| \frac{\partial h(k, x)}{\partial x} \right\| \leq k_b$$

for some $k_b > 0$ and $\forall x \in B_{h'}$

The above results indicate that the system satisfies all the assumptions $B1 - B7$ for a mixed time scale system in [4].

REFERENCES

[1] F. B. Amara, P. T. Kabamba, & A. G. Ulsoy, "Robust adaptive sinusoidal disturbance rejection in linear continuous-time systems," *Proc. of IEEE Conf. Decision Contr.*, pp. 1878–1883, 1997.

[2] F. B. Amara, P. T. Kabamba, & A. G. Ulsoy, "Adaptive sinusoidal disturbance rejection in linear discrete-time systems—part I: theory," *Journal of Dynamic Systems, Measurement, and Control*, vol. 121, pp. 648–654, 1999.

[3] F. B. Amara, P. T. Kabamba, & A. G. Ulsoy, "Adaptive sinusoidal disturbance rejection in linear discrete-time systems—part II: experiments," *Journal of Dynamic Systems, Measurement, and Control*, vol. 121, pp. 655–659, 1999.

[4] E. Bai, L. Fu, & S. Sastry, "Averaging analysis for discrete time and sampled data adaptive systems," *IEEE Trans. on Circuits and Systems*, vol. 35, no. 2, pp. 137–148, 1988.

[5] M. Bodson, J. S. Jensen, & S. C. Douglas, "Active noise control for periodic disturbances," *IEEE Trans. on Control System Technology*, vol. 9, no. 1, pp. 200–205, 2001.

[6] M. Bodson, "Performance of an adaptive algorithm of sinusoidal disturbance rejection in high noise," *Automatica,* vol. 37, no. 7, pp. 1133–1140, 2001.

[7] M. Bodson & S. C. Douglas, "Adaptive algorithms for the rejection of sinusoidal disturbances with unknown frequency," *Automatica,* vol. 33, no. 12, pp. 2213–2221, 1997.

[8] L. J. Brown & Y. Ma, "Identification and cancellation of disturbances having two close sinusoidal components," *Proc. of the American Control Conference*, pp. 4766-4770, 2006.

[9] L. J. Brown & Q. Zhang, "Periodic disturbance cancellation with uncertain frequency," *Automatica,* vol. 40, no. 4, pp. 631–637, 2004.

[10] S. J. Elliott, I. M. Stothers, & P. A. Nelson, "A multiple error LMS algorithm and its application to the active control of sound and vibration," *IEEE Trans. on Acoustics, Speech, and Signal Processing,* vol. 35, no. 10, pp. 1423–1434, 1987.

[11] B. A. Francis & W. M. Wonham, "The internal model principle of control theory," *Automatica,* vol. 12, pp. 457–465, 1976.

[12] J.-J. Fuchs, "Estimating the number of sinusoids in additive white noise," *IEEE Trans. on Acoustics, Speech, and Signal Processing,* vol. 36, no. 12, pp. 1846–1853, 1988.

[13] X. Guo & M. Bodson, "Frequency estimation and tracking of multiple sinusoidal components," *Proc. of IEEE Conf. Decision Contr.,* pp.5360–5365, 2003.

[14] X. Guo & M. Bodson, "Adaptive rejection of disturbances having two sinusoidal components with close and unknown frequencies," *Proc. of the American Control Conference,* pp. 2619–2624, 2005.

[15] S. M. Kuo & D. R. Morgan, *Active noise control systems: algorithms and DSP implementations*, Wiley: New York, NY, 1996.

[16] I. D. Landau, A. Constantinesue, & D. Rey, "Adaptive narrow band disturbance rejection applied to an active suspension—an internal model principle application," *Automatica*, vol. 41, no. 4, pp. 563–574, 2005.

[17] L. Ljung & T. Glad, *Modeling of Dynamic Systems*, Englewood Cliffs: Prentice-Hall, 1993.

[18] K. Maertens, J. Schoukens, K. Deprez, & J. D. De Baerdemaeker, "Development of a smart mass flow sensor based on adaptive notch filtering and frequency domain identification," *Proc. of the American Control Conference*, pp. 4359–4363, 2002.

[19] D. G. Manolakis, V. K. Ingle & S. M. Kogon, *Statistical and adaptive signal processing: spectral estimation, signal modeling, adaptive filtering, and array processing*, McGraw-Hill, Boston, 2000.

[20] R. Marino, G. L. Santosuosso, & P. Tomei, "Robust adaptive compensation of biased sinusoidal disturbances with unknown frequency," *Automatica*, vol. 39, no. 10, pp. 1755–1761, 2003.

[21] R. Marino, G. L. Santosuosso, "Sinusoidal disturbances compensation for a class of nonlinear non-minimum phase stable systems," *Int. Conf. on Control, Automation, Robotics and Vision,* pp. 665–670, 2002.

[22] A. Sacks, M. Bodson, & P. Khosla, "Experimental results of adaptive periodic disturbance cancellation in a high performance magnetic disk drive," *Journal of Dynamic Systems, Measurement, and Control*, vol. 118, pp. 416–424, 1996.

[23] S. Sastry & M. Bodson, *Adaptive control: stability, convergence, and robustness,* Prentice-Hall: Englewood Cliffs, NJ, 1989.

[24] P. Stoica & T. Söderström, "Statistical analysis of MUSIC and subspace rotation estimates of sinusoidal frequencies," *IEEE Trans. on Signal Processing,* vol. 39, no. 8, pp. 1836–1847, 1991.

[25] M. Tomizuka, T.-C. Tsao & K.-K. Chew, "Analysis and synthesis of discrete-time repetitive controllers," *Journal of Dynamic Systems, Measurement, and Control,* vol. 111, pp. 353–358, 1989.

[26] B. Wu & M. Bodson, "A magnitude/phase locked loop approach to parameter estimation of periodic signals," *IEEE Trans. on Automatic Control,* vol. 48, no. 4, pp. 612–618, 2003.

[27] B. Wu & M. Bodson, "Direct adaptive cancellation of periodic disturbances for multivariable plants," *IEEE Trans. on Speech and Audio Processing,* vol. 11, no. 6, pp. 538–548, 2003.

[28] B. Wu & M. Bodson, "Multi-channel active noise control for periodic sources—indirect approach," *Automatica,* vol. 40, no. 2, pp. 203–212, 2004.

[29] Y. Xu, M. de Mathelin, & D. Knittel, "Adaptive rejection of quasi-periodic tension disturbances in the unwinding of a non-circular roll," *Proc. of the American Control Conference*, pp. 4009–4014, 2002.

[30] Z. Zhao & L. L. Brown, "Musical pitch tracking using internal model control based frequency cancellation," *Proc. of IEEE Conf. Decision and Cont.*, pp. 5544–5548, 2003.